Supplement of

Biogeochemical evolution of ponded meltwater in a High Arctic subglacial tunnel

Ashley J. Dubnick[1,2], Rachel L. Spietz[3], Brad D. Danielson[4], Mark L. Skidmore[1], Eric S. Boyd[3], Dave Burgess[4], Charvanaa Dhoonmoon[2], Martin Sharp[2].

[1]Department of Earth Science, Montana State University, Bozeman, Montana, 59717, USA
[2]Department of Earth and Atmospheric Sciences, University of Alberta, Edmonton, Alberta, T6G 2E3, Canada
[3]Department of Microbiology and Cell Biology, Montana State University, Bozeman, MT, 59171, USA
[4]Geological Survey of Canada, 601 Booth Street, Ottawa, Ontario, K1A 0E8, Canada

Correspondence to: Ashley J. Dubnick (ashey.dubnick@montana.edu)

Supplementary Methods S1: Water isotope fractionation model

A model was developed using the principles of isotopic fractionation to estimate the isotopic composition of incremental ice, incremental vapor, and residual water as a hydraulically isolated waterbody progressively freezes and evaporates. Natural waters are composed of hydrogen, which has two stable isotopes (^{1}H and ^{2}H or deuterium, D) and oxygen, which has three stable isotopes (^{16}O, ^{17}O and ^{18}O). H_2O molecules in natural water can therefore have one of nine possible molecular weights. Due to differences in the vibrational energies of the bonds of these molecules, the freezing of water under equilibrium conditions results in heavier molecules fractionating more readily into the solid ice, while lighter molecules fractionate more readily into the remaining liquid water. During evaporation, lighter molecules fractionate more readily into the vapor, leaving the residual water relatively enriched in the heavier molecules.

Eq S1 to Eq S4 were used to (1) determine the freeze:evaporation ratio that yielded $\delta^{18}O$-$\delta^{2}H$ values for incremental ice and residual water close to $\delta^{18}O$-$\delta^{2}H$ values of the ice and water samples measured in this study, and 2) model the evolution of $\delta^{18}O$ and $\delta^{2}H$ of incremental ice, incremental vapor, and residual water as an isolated waterbody progressively freezes and evaporates (at relative rates determined in (1)).

1. **Calculate the isotopic composition of incremental ice (δ_{ii}) at step (i):**

$$\delta_{ii(i)} = \delta_{rw(i-1)} + \varepsilon_{i-w} \quad \text{Eq S1}$$

2. **Calculate the isotopic composition of incremental vapor (δ_{iv}) at step (i):**

$$\delta_{iv(i)} = \delta_{rw(i-1)} - \varepsilon_{w-v} \quad \text{Eq S2}$$

3. **Calculate the isotopic composition of residual water (δ_{rw}) at step (i):**

$$\delta_{rw(i)} = \frac{\delta_{rw(i-1)} - \delta_{ii(i)} \times f - \delta_{iv(i)} \times R \times f}{1 - step - (R \times f)}$$

Eq S3

4. **Calculate the stage of freezing at step (i):**

$$F = (1 - step + R)^i$$

Eq S4

Where:

$\delta_{ii(i)}$ is the isotopic composition of the incremental ice at step (i).

$\delta_{rw(i-1)}$ is the isotopic composition of the residual water at the prior step (*i-1*). Initial δ_{rw} was set to the average isotopic composition of channel ice.

ε_{i-w} is the isotopic difference between ice and water phases (derived as the average at sites 8-9; Table S1)

$\delta_{iv(i)}$ is the isotopic composition of the incremental vapor at step (i)

ε_{w-v} is the isotopic difference between the water and vapor phases. ε_{w-v} was set to rates derived for evaporation at 0°C (1.01173 for $\delta^{18}O$ and 1.11255 for $\delta^{2}H$) (Majoube, 1971).

$\delta_{rw(i)}$ is the isotopic composition of the residual water at step (*i*).

f is the fraction of the pond that is frozen in each step of the model (0.1%).

R is the ratio of evaporation:freezing and is specified by the user. R was adjusted to optimize the model's fit with the $\delta^{2}H$-$\delta^{18}O$ of observed channel ice, pond ice and pond water samples (0.025).

F is the cumulative fraction of the water that remains residual at step (i).

Supplementary Methods S2: Cl^- and geochemical model

Eq S5 to Eq S9 were used to (1) calculate $[Cl^-]$ in incremental ice and residual water as an isolated waterbody progressively freezes and evaporates, to determine the stage of freezing affiliated with each sample site in the pond, and (2) calculate the concentration of other biogeochemical parameters in incremental ice and residual water as an isolated waterbody freezes to those extents.

1. **Calculate the effective segregation coefficients $K_{eff(x)}$ for biogeochemical species (*X*):**

$$K_{eff(X)} = \frac{[\bar{X}]_{ice}}{[\bar{X}]_{water}}$$ Eq S5

2. **Calculate the concentration of biogeochemical species (*X*) in the incremental ice at step (i):**

$$[X]_{ii(i)} = [X]_{rw(i-1)} \times K_{eff(X)}$$ Eq S6

3. **Calculate the concentration of biogeochemical species (*X*) in the residual water at step (i):**

$$[X]_{rw(i)} = \frac{[X]_{rw(i-1)} - [X]_{ii(i)} \times f}{1 - f - (R \times f)} \quad \text{Eq S7}$$

4. **Calculate the stage of freezing at step (i):**

$$F = (1 - f + R)^i \quad \text{Eq S8}$$

Where:

$K_{eff(x)}$ is the effective segregation coefficient for biogeochemical species X,

$[\bar{X}]_{ice}$ is the average concentration of species X in the ice at sites 8 and 9

$[\bar{X}]_{water}$ is the average concentration of species X in the water at sites 8 and 9

$[X]_{ii(i)}$ is the concentration of species X in the incremental ice (*ii*) at step (*i*)

$[X]_{rw(i)}$ is the concentration of species X in the residual water (*rw*) at step (*i*)

$[X]_{rw(i-1)}$ is the concentration of species X in the residual water (*rw*) at the prior step (i-1). Initial $[X]_{rw}$ was set to the average concentration of species X among channel ice samples.

f is the step interval, represented as the fraction of the pond water that is frozen in each step of the model (0.1%).

R is the ratio of evaporation: freezing (derived from the isotope model; 0.025)

F is the cumulative fraction of water that remains residual at step (*i*).

Supplementary Methods S3: Hydraulic head calculations

Hydraulic head quantifies the mechanical energy of a fluid. Previous studies have found that the subglacial drainage structure of polythermal glaciers corresponds to subglacial hydraulic potential, in which water flows from high hydraulic head to low hydraulic head (Hagen et al., 2000; Pälli et al., 2003; Rippin et al., 2003). Hydraulic head was calculated assuming that the subglacial water pressure is equal to the ice overburden pressure (Hagen et al., 2000; Pälli et al., 2003; Rippin et al., 2003):

$$h = S\frac{\rho_i}{\rho_b} + B(1 - \frac{\rho_i}{\rho_b}) \quad \text{Eq S9}$$

where h is the hydraulic head, S is the surface elevation, ρ_i is the ice density (917 kg/m3) and ρ_b is the water density (1000 kg/m3), and B is the bed elevation. Surface and bed elevation measurements were derived from airborne radar and laser altimeter transect collected by Operation IceBridge along a cross-sectional profile of the Sverdrup Glacier approximately 100 m north of the tunnel endpoint (Figure 1) (Paden et al., 2019).

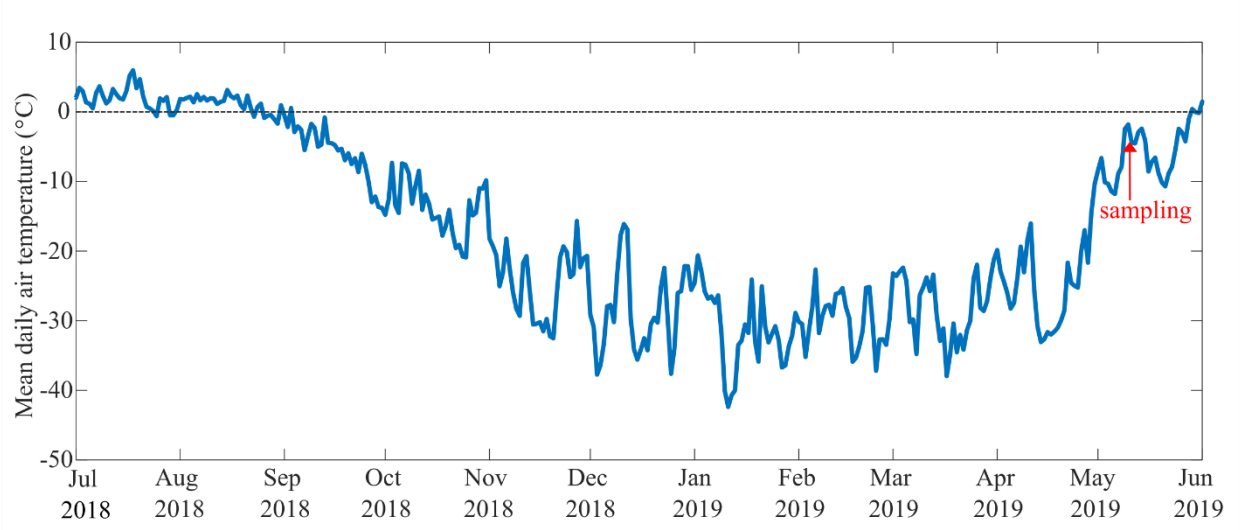

Figure S1: Air temperature data were recorded hourly (averaged to daily) on a CR1000 data logger at an automatic weather station (75° 41'N, 83° 15W, 330 m a.s.l.) on the Sverdrup Glacier. All measurements were collected with a Campbell Scientific thermilinear temperature probe nominally mounted ~2 m above the ice cap surface in an RM Young radiation shield (Burgess, 2017)

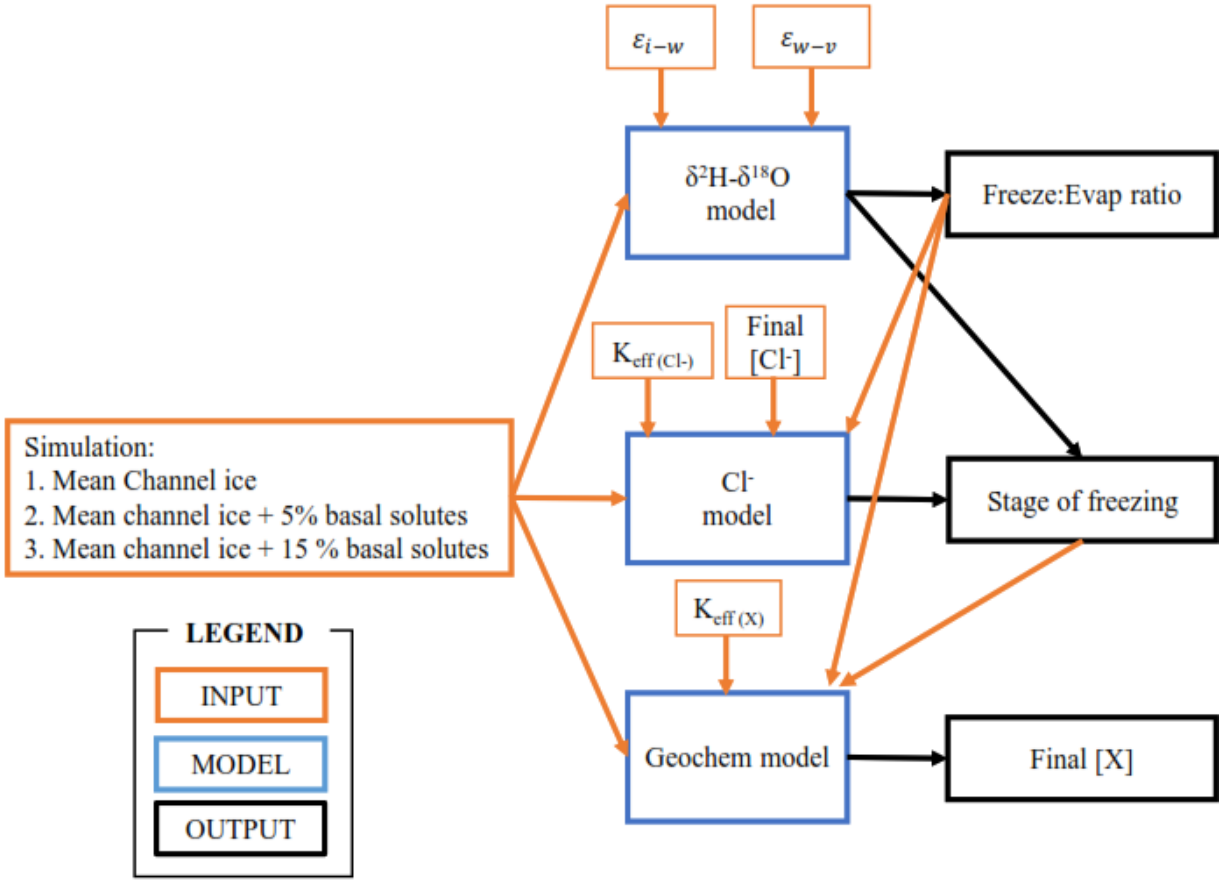

Figure S2: Schematic showing integration of the isotope, Cl^-, and geochemical models and the three simulation conditions

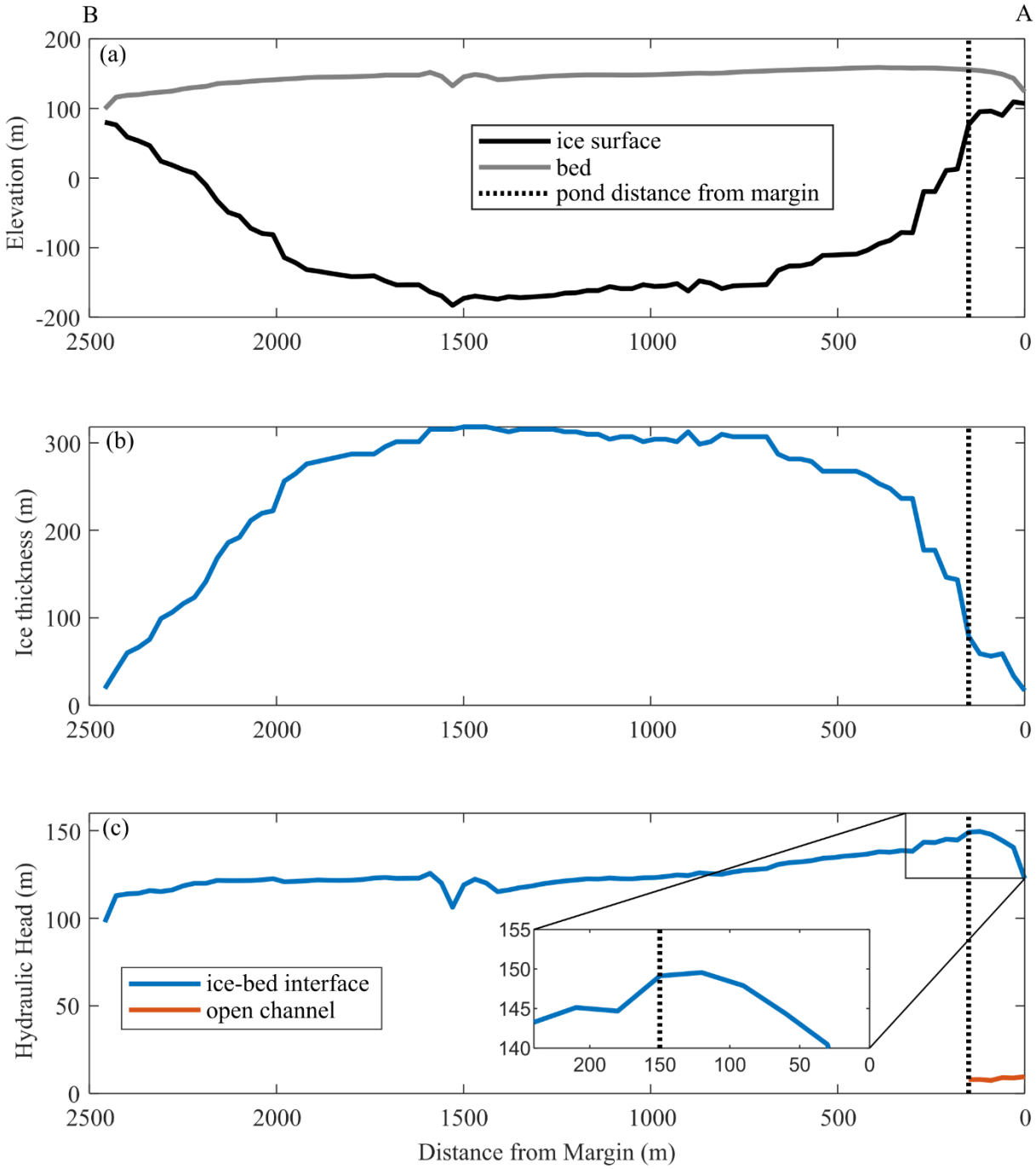

Figure S3: (a) Sverdrup glacier cross section as presented in Figure 1 (a) using elevations from (Paden et al., 2019), (b) ice thickness across this profile, and (c) hydraulic head across this profile. Dotted vertical lines in all panels indicate the subglacial pond's distance from the ice margin.

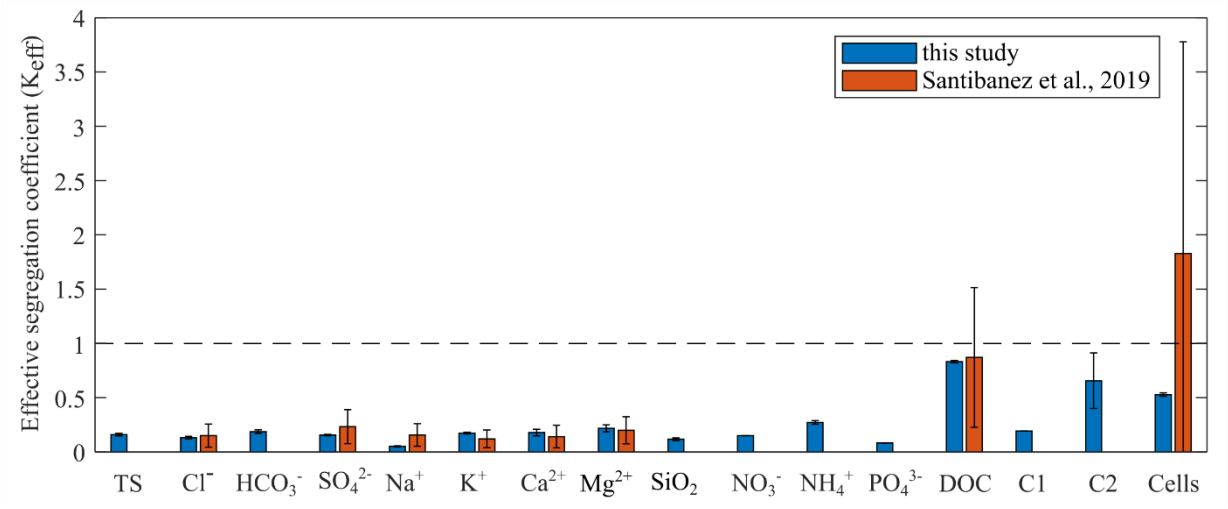

Figure S4: Effective segregation coefficients (K_{eff}) used for geochemical modeling in this study compared to mean K_{eff} values derived from four mesocosm experiments using water from perennially (Antarctic) and seasonally (Alaska and Montana, USA) ice-covered lakes (Santibáñez et al., 2019). Error bars represent 1 standard deviation. Note TS, HCO_3^-, SiO_2, NO_3^-, NH_4^+, PO_4^{3-}, and C1 and C2 fluorescence were not included in the study by Santibanze et al. (2019).

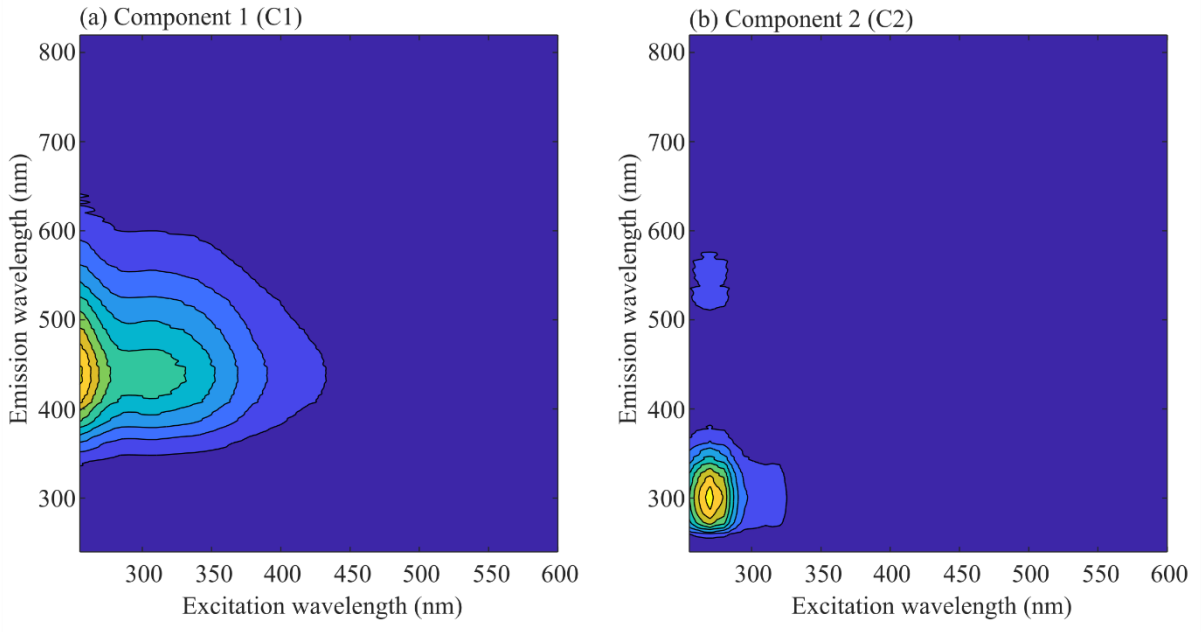

Figure S5: PARAFAC components including (a) component 1 (C1) with peak excitation wavelength of <255 nm and peak excitation wavelength of 445 nm, and (b) component 2 (C2) with peak excitation wavelength of 270 nm and peak emission wavelength of 300 nm.

Table S1: Typical δ^2H and $\delta^{18}O$ equilibrium values for freezing compared to those derived in this study.

	$\delta^{18}O$	**δ^2H**	**Reference**
Fast freeze	1.0005	1.007	Ferrick et al. (2002)
Slow Freeze	1.0027	1.015	Ferrick et al. (2002)
Vostok ice-water interface	1.0031	1.0208	Jouzel et al. (1999)
Sverdrup subglacial tunnel - pond slush	1.0018	1.0109	This study

References

Burgess, D. O.: Mass balance of ice caps in the Queen Elizabeth Islands, Arctic Canada, https://doi.org/10.4095/300231, 2017.

Ferrick, M. G., Calkins, D. J., Perron, N. M., Cragin, J. H., and Kendall, C.: Diffusion model validation and interpretation of stable isotopes in river and lake ice, Hydrol. Process., 16, 851–872, 2002.

Hagen, J. O., Etzelmüller, B., and Nuttall, A.-M.: Runoff and drainage pattern derived from digital elevation models, Finsterwalderbreen, Svalbard, Ann. Glaciol., 31, 147–152, https://doi.org/DOI: 10.3189/172756400781819879, 2000.

Jouzel, J., Petit, J. R., Souchez, R., Barkov, N. I., Lipenkov, V. Y., Raynaud, D., Stievenard, M., Vassiliev, N. I., Verbeke, V., and Vimeux, F.: More than 200 meters of lake ice above subglacial Lake Vostok, Antarctica, Science (80-.)., 286, 2138–2141, https://doi.org/10.1126/science.286.5447.2138, 1999.

Majoube, M.: fractionnement en oxygéne-18 et en deuterium entre l'eau et la vapeur, J. Chim. Phys., 68, 1423–1436, 1971.

Paden, J., Li, J., Leuschen, C., Rodriguez-Morales, F., and Hale, R.: IceBridge MCoRDS L2 Ice Thickness, Version 1, https://doi.org/https://doi.org/10.5067/GDQ0CUCVTE2Q, 2019, 2019.

Pälli, A., Moore, J. C., Jania, J., Kolondra, L., and Glowacki, P.: The drainage pattern of Hansbreen and Werenskioldbreen, two polythermal glaciers in Svalbard, Polar Res., 22, 355–371, https://doi.org/10.3402/polar.v22i2.6465, 2003.

Rippin, D., Willis, I., Arnold, N., Hodson, A., Moore, J., Kohler, J., and Björnsson, H.: Changes in geometry and subglacial drainage of midre Lovénbreen, Svalbard, determined from digital elevation models, Earth Surf. Process. Landforms, 28, 273–298, https://doi.org/10.1002/esp.485, 2003.

Santibáñez, P. A., Michaud, A. B., Vick-Majors, T. J., D'Andrilli, J., Chiuchiolo, A., Hand, K. P., and Priscu, J. C.: Differential incorporation of bacteria, organic matter, and inorganic ions into lake ice during ice formation, J. Geophys. Res. Biogeosciences, 124, 585–600, https://doi.org/10.1029/2018JG004825, 2019.